Analyst

PAPER

Cite this: *Analyst*, 2019, **144**, 4545

Fluorescent visual quantitation of cell-secreted sialoglycoconjugates by chemoselective recognition and hybridization chain reaction†

Yingying Xiong,‡[a] Yunlong Chen,‡[a] Lin Ding,[a] Xiaoqiang Liu[b] and Huangxian Ju*[a]

Received 29th March 2019,
Accepted 7th June 2019

DOI: 10.1039/c9an00572b

rsc.li/analyst

Sialic acid (SA), usually located at the termini of glycan chains, is one of the most important monosaccharide blocks for glycosylation of proteins. The expression level of sialoglycoconjugates (SiaGCs) in cellular secretome is of great significance in diagnosis of tumor malignancy. This work developed a fluorescent visual method for the detection of SiaGCs secreted from living cells by a boronic acid modified chip based chemoselective recognition and hybridization chain reaction. The cell-secreted SiaGCs, which were labeled with the azide group through a metabolic labeling technique during cell culture, were captured by the chip through chemoselective recognition of boronic acid toward SA. After further conjugating the azide group with an alkyne modified DNA probe, the captured SiaGCs could be conveniently endowed with the amplified fluorescent signal through a hybridization chain reaction of a pair of dye-labeled DNA hairpins, which led to a quantitative imaging method for detection of SiaGCs. The average amount of metabolically labeled SiaGCs secreted from a single HeLa cell and MCF-7 cell was 2.18×10^{-17} and 3.98×10^{-17} mol, respectively. The proposed method could be utilized to monitor the variation of the secreted SiaGCs during drug treatment, providing a useful tool for investigating the glycosylation and glycan-related biological processes.

Introduction

The extracellular matrix (ECM) is a dynamic and complex three-dimensional macromolecular network existing in all tissues and organs. The major constituents of the ECM include elastin, collagens, fibronectin, laminins, proteoglycans, glycosaminoglycans, and other glycoproteins, which provide spatial context and structural support for signaling events and cell proliferation.[1–3] Most secreted proteins are decorated with a dense and complex array of glycan chains, which are involved in the ECM to regulate diverse cellular physiological processes, including cell growth, proliferation, differentiation, migration, homeostasis and morphogenesis.[4–9] Therefore, abnormities of glycosylation on secreted proteins are associated with the initiation and progression of many diseases, such as fibrosis and cancer, which suggests that glycans on secreted proteins can act as potential targets for disease diagnosis and pharmacological treatment.[3,10,11]

Among various glycoconjugates, sialoglycoconjugates (SiaGCs), which possess terminal sialic acids (SAs),[12,13] are of vital importance due to their role in mediation and modulation of a series of physiological and pathological processes.[5,14,15] The total SiaGC content in the serum has been detected to predict the risk of various diseases, including coronary heart disease and cardiovascular disease.[16–18] Cancer cells often aberrantly display an increase in overall sialylation compared with their normal counterparts,[14,19] leading to excessive secretion of SiaGCs.[20–24] Thus, the detection of SiaGCs in cellular secretome can provide a comprehensive understanding of cell status with abnormal cell metabolism and malignant tumor progression.

The current detection methods for glycoprotein-related cellular secretome mainly focus on extraction and identification of the glycosylated proteins.[13,25,26] These methods need to modify the carbohydrates with chemical oxidants or biological enzymes and then separate the glycosylated proteins by chemical affinity selection, which causes a considerable loss of glycan expression information. Besides, most of them can only

[a]*State Key Laboratory of Analytical Chemistry for Life Science, School of Chemistry and Chemical Engineering, Nanjing University, Nanjing 210023, China. E-mail: hxju@nju.edu.cn*
[b]*College of Chemistry and Chemical Engineering, Henan University, Kaifeng, Henan Province, 475004, P.R. China*

†Electronic supplementary information (ESI) available: NMR spectra, gel electrophoresis image, fluorescent images of metabolically labeled SiaGCs and azide-modified SA, sequences of oligonucleotides. See DOI: 10.1039/c9an00572b

‡These authors contributed equally to this work.

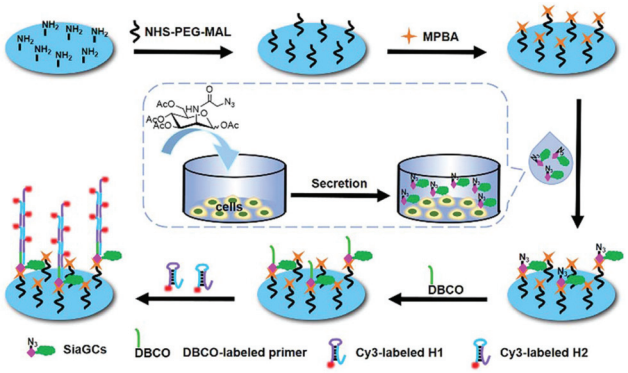

Scheme 1 Schematic illustration of detection of SiaGCs secreted from cells.

give a qualitative description of the glycan in cellular secretome, and a quantitative method for one specific carbohydrate-containing compound secreted from cells is still an urgent demand. This work developed a fluorescent visual strategy for quantification of metabolically labeled SiaGCs in cellular secretome.

In order to avoid the complex sample handling and the loss of SA information, the proposed method firstly labeled the SAs in living cells with the azide group through a metabolic labeling technique (Scheme 1). Owing to the small size, the azide group will cause negligible influence on cellular physiology.[12,27,28] The secreted SiaGCs could be conveniently captured with a phenyl boric acid (PBA) modified chip through the chemoselective conjugation between PBA and SA[29–34] to generate fluorescent signals by conjugating the azide group with an alkyne modified DNA probe and then performing a hybridization chain reaction (HCR) for signal amplification. The fluorescent image was then obtained to quantify the amount of SiaGCs in the cellular secretome. The designed strategy successfully achieved the visual quantification of metabolically labeled SiaGCs secreted from different types of cells and the variation monitoring of SiaGCs during drug treatment. Thus, this work provides a useful quantification tool for uncovering glycan-secretion related biological processes.

Experimental

Materials and reagents

4-Mercaptophenyl boronic acid (MPBA), succinimidyl ester-PEG 3400-maleimide (NHS-PEG 3400-Mal, ≥99%), sialic acid (SA), 4-(4,6-dimethoxy-1,3,5-triazin-2-yl)-4-methylmorpholin-4-ium chloride (DMTMM, ≥96.0%), dibenzocyclooctyne-Cy3 (DBCO-Cy3), 3-azidopropan-1-amine, ion-exchange resin IR-120 and bovine serum albumin (BSA) were purchased from Sigma-Aldrich, Inc. (USA). Fetal bovine serum (FBS), streptomycin, penicillin and tetraacetylated *N*-azidoacetyl-D-mannosamine (Ac4ManNAz) were obtained from Thermo Fisher Scientific (USA). Triethylamine, ethanol, methanol (MeOH), trichloromethane ($CHCl_3$), acetic anhydride (Ac_2O), ethyl acetate (EtOAc), sodium methoxide (MeONa) and pyridine were provided by J&K Technology Co., Ltd (China). Sambucus nigra agglutinin (SNA) was purchased from Vector Laboratories (USA). α2-3,6,8,9 Neuraminidase A (sialidase) was purchased from New England Biolabs, Inc. (USA). Tunicamycin (TM) was provided by Abcam PLC Co., Ltd (USA). The amino-modified glass slides were purchased from Shanghai Baio Technology Co., Ltd (China). Cell culture media such as RPMI-1640, Dulbecco's modified Eagle's medium (DMEM), phosphate buffered saline (pH 7.4, containing 136.7 mM NaCl, 2.7 mM KCl, 8.72 mM Na_2HPO_4, 1.41 mM KH_2PO_4, 1 mM $MgCl_2$, and 1 mM $CaCl_2$), and HeLa, HaCaT, MCF-7 and MCF-10A cell lines were purchased from KeyGEN Biotech Co., Ltd (Nanjing, China). All DNA sequences shown in Table S1† were customized from Sangon Biological Engineering Technology & Co. Ltd (Shanghai, China). Tris–EDTA buffer (TE) containing 10 mM Tris–HCl and 1 mM EDTA (pH 8.0) was used as DNA stock solution. HCR hybridization buffer was prepared by adding 100 mM NaCl and 10 mM $MgCl_2$ in TE. All other reagents were of analytical grade. All aqueous solutions were prepared using ultrapure water (≥18 MΩ, Milli-Q, Millipore).

Apparatus

The chip was scanned with a Biochip Analysis System (Capitalbio, China). The fluorescence cell images were obtained with a TCS SP8 confocal laser scanning microscope (CLSM) (Leica, Germany). Native polyacrylamide gel electrophoresis (PAGE) was performed on an Electrophoresis Analyzer (Bio-Rad, USA) and imaged on a Bio-Rad ChemDoc XRS facility (Bio-Rad, USA). Contact angle measurements were performed on an OCA30 Video Optical Contact Angle Measuring Instrument (Dataphysics Instruments Gmb, USA). ^{1}H NMR was recorded on an FT AM 400 (400 MHz). Chemical shifts were reported in parts per million (ppm) referenced to the appropriate solvent peak or 0.0 ppm for tetramethylsilane. The fully decoupled ^{13}C NMR was recorded on an FT AM 400 (101 MHz). The mass spectrum was obtained by using a SHIMAZU LCMS-2020. The cells numbers were calculated using a Countess II FL Automated Cell Counter (Life Technologies, USA).

Cell culture

HeLa and HaCaT cell lines were cultured at 37 °C in high-glucose Dulbecco's modified Eagle's medium (DMEM) supplemented with 10% fetal bovine serum, penicillin (100 μg mL^{-1}), and streptomycin (100 μg mL^{-1}) in a humidified atmosphere containing 5% CO_2. MCF-7 and MCF-10A cell lines were cultured in RPMI 1640 medium (GIBCO) supplemented with 10% fetal bovine serum, penicillin (100 μg mL^{-1}), and streptomycin (100 μg mL^{-1}) at 37 °C with 5% CO_2.

Preparation of capture chip

An array containing 75 identical holes (15 rows × 5 columns) was designed on a single amino-modified glass slide. The dia-

meter of each hole was 2 mm. 10 mM NHS-PEG 3400-Mal was added in each hole and incubated at 37 °C for 6 hours. After the slide was thoroughly washed with ultrapure water and dried with nitrogen stream, it was immersed in 10 mM MPBA in ethanol containing 0.1% triethylamine and vibrated for 2 h at room temperature. The unreacted groups were blocked with 20% BSA in PBS for 1 h at 37 °C.[35,36] After washing thoroughly with ultrapure water and drying with a nitrogen stream, the capture chip was kept at 4 °C for further use.

Metabolic labeling of sialic acid

HeLa cells were seeded in sterilized dishes and cultured overnight. They were then incubated in fresh culture medium containing 40 μM Ac_4ManNAz for another 2 days. In order to demonstrate the successful labeling, these cells were washed with 1% FBS-containing PBS and treated with 10 μM DBCO-Cy3 for 30 min at 4 °C. They were then carefully washed with PBS to perform the imaging with CLSM.

Profiling of SiaGCs

After Ac_4ManNAz treated HeLa cells were cultured in 700 μL PBS for 6 h, the PBS containing the secreted SiaGCs was collected as the cellular secretion. The number of HeLa cells in Petri dishes was calculated by Cell Counters. The cellular secretions from HaCaT cells, MCF-7 cells and MCF-10A cells were obtained with the same procedure. HCR hairpins H1 and H2 were dissolved in 50 μL HCR hybridization buffer, respectively. Then the solutions were annealed in a thermocycler with the temperature rising rapidly to 95 °C and subsequently dropping slowly to 25 °C in approximately 3 h. The solutions were stored at 4 °C for future use.

As shown in Scheme 1, 2 μL of cellular secretion was added into each hole of the capture chip and incubated at 37 °C for 4 h. After the chip was washed with water thrice and dried with nitrogen stream, 2 μL of 10 μM DBCO-labeled HCR primer was added into the holes and incubated at 4 °C for 30 min to perform the click reaction. The chip was then washed thoroughly with ultrapure water and dried with nitrogen stream, and 2 μL of the mixture of 10 μM annealed HCR hairpins H1 and H2 in HCR buffer was added into each hole and incubated at 37 °C for 2 h to perform HCR amplification. After the chip was thoroughly washed with 0.05% tween 20 and dried with nitrogen stream, it was submitted to a biochip analysis system to measure the fluorescence signals. The mean fluorescence intensity (I) of each hole was automatically recorded and represented by color scale for data processing, which ranged from 0 to 65 535.

Synthesis of azide-modified sialic acid

The azide-modified sialic acid was firstly synthesized with an improved method as shown in Scheme 2.[37–40] The SA (800 mg) was heated with Ac_2O (20 mL) and pyridine (20 mL) at 60 °C for 2 h. The reaction mixture was concentrated *in vacuo* to give protected SA (1250 mg, 93%). The protected SA (0.8 mmol, 415.6 mg) and DMTMM (2 mmol, 553.4 mg) were dissolved in 8 mL MeOH in a 25 mL Schlenk flask equipped with a magnetic bar. 3-Azidopropan-1-amine (2.4 mmol, 240 mg) was added dropwise to the solution, and the mixture was allowed to stir for 3 h at room temperature under nitrogen atmosphere. The solution was concentrated under vacuum and purified using a flash chromatography column (EtOAc) to obtain the azide-modified SA as white solid (330 mg, with a yield of 69%), which was dissolved in 10 mL MeOH in a 25 mL Schlenk flask equipped with a magnetic bar. After 0.4 mL MeONa (5 M in MeOH) was added dropwise, the mixture was allowed to stir for 8 h at room temperature and acidized by ion-exchange resin IR-120. The mixture was filtered, and the filtrate was concentrated under vacuum, purified using a flash chromatography column ($CHCl_3$: MeOH : H_2O = 6 : 4 : 1) to obtain the pure azide-modified SA as white solid (125.2 mg, with a yield of 58%).

Remodeling of *N*-glycosylation with tunicamycin treatment

Four kinds of cell lines were seeded at the same concentration and cultured overnight, washed three times with PBS, and then treated with the mixture of Ac_4ManNAz (40 μM) and TM (100 nM) in a 5% CO_2 incubator at 37 °C for 48 h. The controlled trials were performed with an identical procedure without TM treatment. The collected cellular secretion was added into each hole of the capture chip to perform the visual detection. The variation of fluorescence intensity upon TM treatment was analyzed by one-way ANOVA.

Results and discussion

Characterization of capture chip

The contact angle images of glass slides modified with amino group (40.1°), MAL (61.4°) and MPBA (75.3°) showed the increasing hydrophobicity of amino group, maleimide and

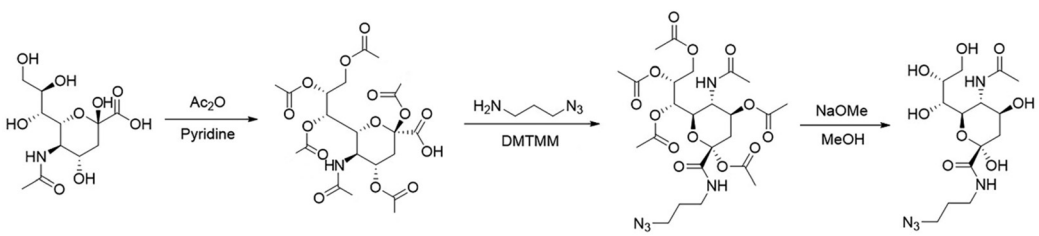

Scheme 2 Synthesis of azide-modified sialic acid.

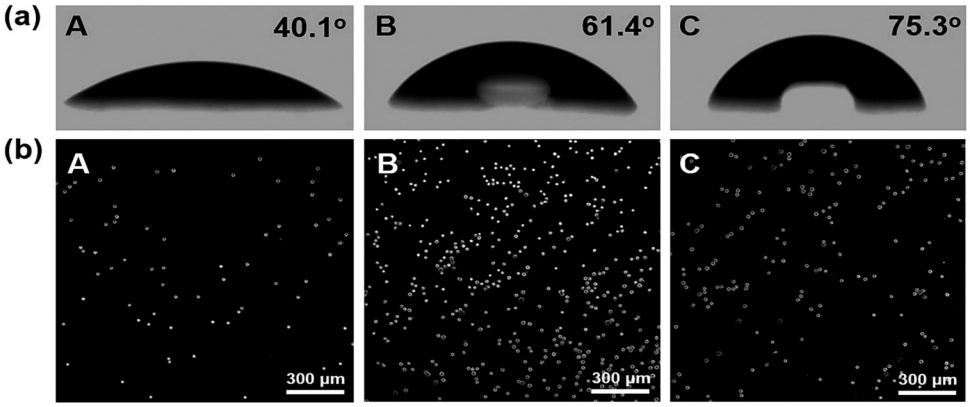

Fig. 1 (a) Contact angle images of the glass slide modified with amino group (A), maleimide (MAL) (B) and 4-mercaptophenyl boronic acid (MPBA) (C). (b) Comparison of capture ability for untreated HeLa cells at (A) MAL- and (B) MPBA-modified glass slides, and (C) sialidase-treated HeLa cells at the MPBA-modified glass slide. Scale bar: 300 μm.

phenylboronic groups (Fig. 1a), which confirmed the successful chip modification. These modified chips showed different cell capturing abilities (Fig. 1b). The MPBA-modified glass slide could capture more suspended HeLa cells than the MAL-modified chip, while sialidase-treated suspended HeLa cells showed lower loading, indicating the chemoselective recognition of MPBA to SA on the prepared capture slides.

Characterization of azide-modified sialic acid

After the synthesized azide-modified sialic acid was purified with column chromatography (chloroform/methanol/water = 6 : 4 : 1, R_f = 0.45), it showed the following characteristics: molecular weight 390.15 (Fig. S1†); ^{1}H NMR (400 MHz, deuterium oxide) δ 4.02–3.91 (m, 1H), 3.88–3.74 (m, 2H), 3.72–3.65 (m, 1H), 3.64–3.43 (m, 2H), 3.42–3.21 (m, 5H), 2.29–1.90 (m, 5H) and 1.81–1.69 (m, 2H) (Fig. S2†); ^{13}C NMR (101 MHz, deuterium oxide) δ 174.91, 172.66, 95.56, 70.48, 70.13, 68.25, 66.75, 63.17, 52.14, 48.79, 39.60, 36.81, 27.48 and 22.09 (Fig. S3†). These characteristics confirmed the successful synthesis and purification of azide-modified SA.

Metabolic labeling of cellular SiaGCs

DBCO-Cy3 was used to validate the metabolic labeling of cellular SiaGCs. After HeLa cells were treated with Ac_4ManNAz, they exhibited obvious fluorescence of Cy3, while HeLa cells without Ac_4ManNAz treatment did not show any response (Fig. 2), indicating the feasibility of metabolic labeling of cellular SiaGCs.

Feasibility of HCR amplification for fluorescent visual analysis

HCR amplification can produce a long double-strand DNA with an amplified fluorescence signal readout.[41,42] It was verified with gel electrophoresis, which showed the good purity of annealed HCR hairpins H1 and H2, and the efficiency of HCR in the presence of HCR primer (Fig. S4†).

In order to improve the sensitivity, 20% BSA was employed to block the capture chip and reduce nonspecific adsorption.

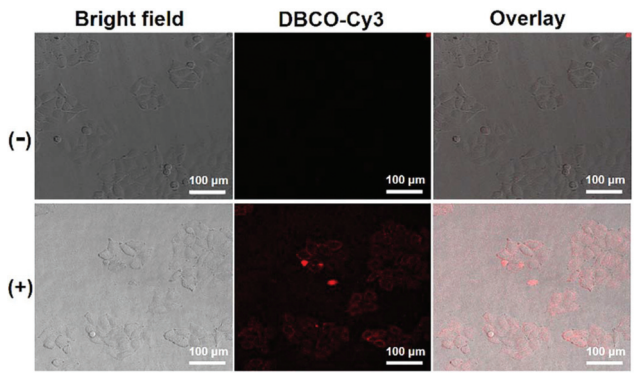

Fig. 2 Validation of metabolic glycan labeling in HeLa cells before (–) and after (+) Ac_4ManNAz treatment. Scale bar: 100 μm.

After the cellular secretion from Ac_4ManNAz-treated HeLa cells was added into the holes of the capture chip, the click reaction and HCR amplification were performed with a DBCO-labeled primer and then HCR hairpins H1 and H2, which produced a fluorescence signal 17.8 times higher than that without HCR (A and B in Fig. 3), while no fluorescent signal was observed from the cellular secretion of HeLa cells without metabolic labeling (C in Fig. 3), which excluded the nonspecific absorption of the DNA probe and demonstrated the successful HCR amplification on the capture chip.

The alkynyl-mediated click conjugation of the DBCO-labeled primer to the azide-modified SA captured on the chip was further demonstrated. As shown in D in Fig. 3, in the absence of DBCO, the signal was almost indiscernible. After the cellular secretion was treated with 10 μg mL^{-1} SNA at 37 °C for 1 h to block the SA group,[43,44] a significant decrease of the fluorescence signal was observed (E in Fig. 3), which further confirmed the SA-mediated chemoselective capturing process. All of these results validated the feasibility of the proposed method for the detection of SiaGCs secreted from living cells.

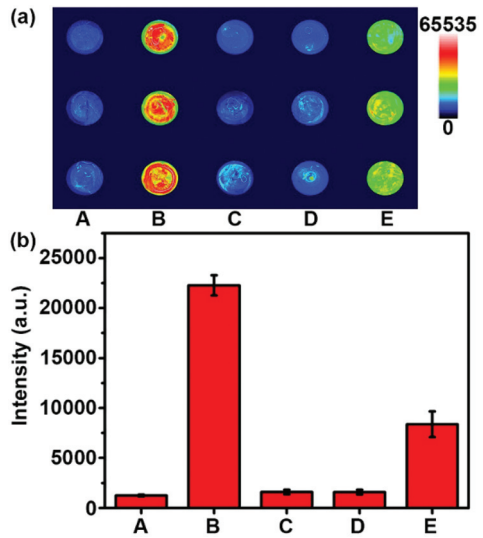

Fig. 3 (a) Fluorescent image of Ac_4ManNAz-labeled SiaGCs secreted from HeLa cells at MPBA-modified glass slide before (A) and after (B) HCR, (C) unlabeled SiaGCs with the same procedure as B, (D) B with replacement of the DBCO-labeled primer by the DBCO-unlabeled primer and (E) B with an additional step of incubating SiaGCs with SNA before capture. (b) Corresponding fluorescent intensity.

Detection performance

The incubation time of the cellular secretion for capturing SiaGCs to the chip was optimized to be 4 h (Fig. S5†). The secretions from two kinds of cancer cells, HeLa cells and MCF-7 cells, and their corresponding normal cells, HaCaT cells and MCF-10A cells, were detected under optimal conditions, respectively (Fig. 4). After these cells were treated with Ac_4ManNAz and then incubated with fresh PBS for 6 h to collect the cellular secretion, the detection procedure was performed to record the fluorescent signals. The fluorescence intensity for HeLa and MCF-7 cells exhibited a rapid increase along with the increasing cell number to 1.8×10^5 cells per mL. The slow increase at the high cell number was attributed to the limited capture sites on the chip. In contrast, the fluorescence signal for HaCaT and MCF-10A cells was much weaker, indicating the overexpression of SiaGCs in cancer cells.

Thus, the proposed method could distinguish between cancer cells and their corresponding normal cells well. At the low concentration range, the fluorescence intensity was proportional to the number of HeLa and MCF-7 cells (Fig. 4, the white frame), which showed the linearity in 33 to 520 cells per hole for HeLa cells and 25 to 320 cells per hole for MCF-7 cells (Fig. S6†) as shown in eqn (1):

$$I = k_1 \times n_{\text{cell}} + b_1 \quad (1)$$

where the corresponding k_1 and b_1 are 30.7 and 819.6 for HeLa cells and 56.2 and 1023 for MCF-7 cells, respectively.

In order to quantify the metabolically labeled SiaGCs secreted from living cells, the calibration curve was obtained with the synthetic azide-modified SA on the capture chip (Fig. S7†), which showed linearity in the range from 0.4 to 16 fmol ($R = 0.998$) as shown in the following linear equation:

$$I = k_2 \times n_{\text{SA-N3}} + b_2 \quad (2)$$

where the corresponding k_2 and b_2 are 1411 and 1261, respectively.

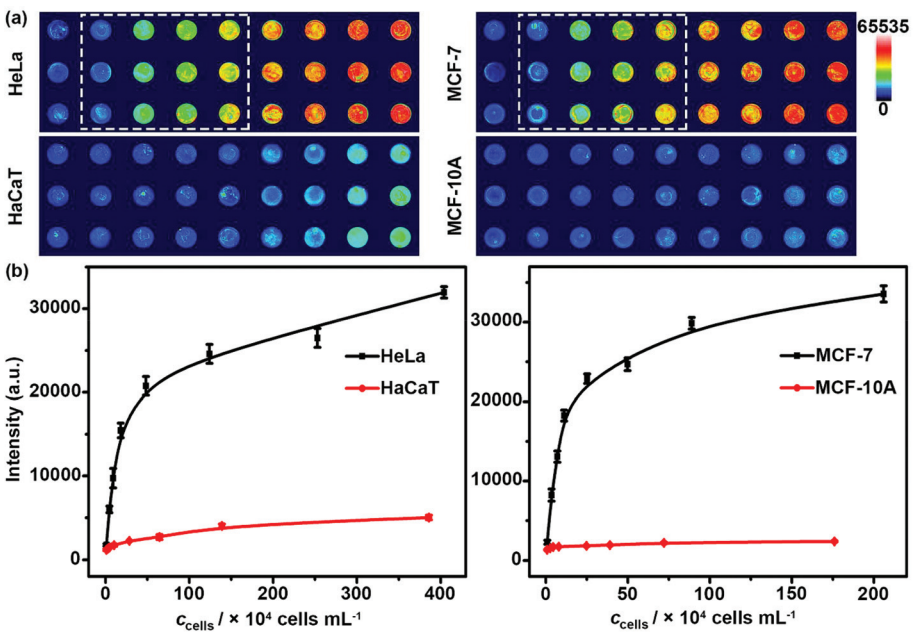

Fig. 4 (a) Fluorescent images of metabolically labeled SiaGCs secreted from different concentrations of HeLa, HaCaT, MCF-7 and MCF-10A cells, and (b) plots of fluorescent intensity *vs.* cell concentration.

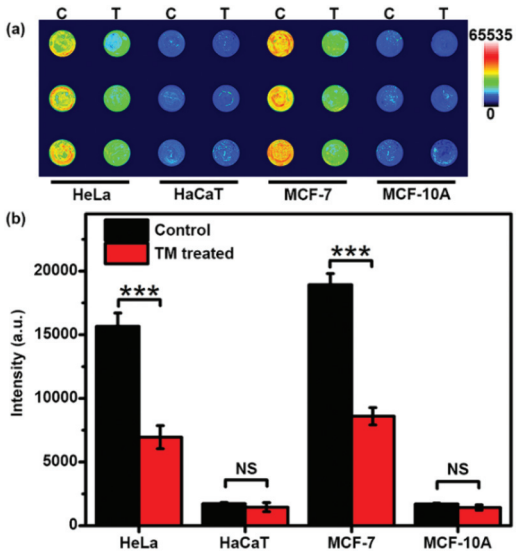

Fig. 5 (a) Fluorescent image and (b) histogram for secreted SiaGCs from four kinds of cells. C and T indicate spots without and with TM treatment, respectively. Statistical analysis in (b): *t*-test (***$p < 0.001$; NS, not significant).

Considering the low background, which resulted in the relatively low values of b_1 and b_2, the average amount of metabolically labeled SiaGCs secreted from each cell could be assumed from eqn (1) and (2) with eqn (3):

$$k = k_1/k_2. \quad (3)$$

The metabolically labeled SiaGCs from a single HeLa cell and MCF-7 cell were 2.18×10^{-17} mol and 3.98×10^{-17} mol, respectively.

Monitoring of secreted SiaGCs

The glycosylated proteins in cellular secretome are mainly posttranslationally modified with N-linked glycans.[12,13] Tunicamycin (TM) can act as an *N*-glycosylation inhibitor to affect the glycosylation level of secretome, but it does not affect cell growth or morphology.[45–48] Thus, TM was used to treat the cells for regulating the level of secreted SiaGCs. After TM treatment, the fluorescence intensity for HeLa and MCF-7 cells decreased significantly (Fig. 5), which could be attributed to the inhibition of *N*-glycan residues, while the change of fluorescence intensity for HaCaT and MCF-10A cells upon the TM treatment was insignificant (Fig. 5b). This result further verified the specificity of the designed strategy and proved the practicality of the proposed strategy as a platform for monitoring the secreted SiaGCs from different cell lines.

Conclusions

This work proposes a fluorescent visual method for the quantitation of metabolically labeled SiaGCs secreted from living cells. The secreted target SiaGCs can be conveniently captured by a boronic acid modified chip through chemoselective recognition and be translated to fluorescent signals with an alkyne modified DNA probe to initiate the HCR amplification. The amplified visual signal can be used to quantify the amount of metabolically labeled SiaGCs secreted from a single cell with a calibration curve. The proposed method can also be used for distinguishing the cancer cells from normal cells and monitoring the variation of the secreted SiaGCs during drug treatment, underlining its promising application.

Conflicts of interest

There are no conflicts to declare.

Acknowledgements

This work was financially supported by the National Natural Science Foundation of China (21635005, 21827812, 21890741) and Natural Science Foundation of Jiangsu Province (BK20160646).

Notes and references

1 S. H. Kim, J. Turnbull and S. Guimond, *J. Endocrinol.*, 2011, **209**, 139–151.
2 A. D. Theocharis, S. S. Skandalis, C. Gialeli and N. K. Karamanos, *Adv. Drug Delivery Rev.*, 2016, **97**, 4–27.
3 C. Bonnans, J. Chou and Z. Werb, *Nat. Rev. Mol. Cell Biol.*, 2014, **15**, 786–801.
4 M. Uhlén, L. Fagerberg, B. M. Hallström, C. Lindskog, P. Oksvold, A. Mardinoglu, Å. Sivertsson, C. Kampf, E. Sjöstedt, A. Asplund, I. Olsson, K. Edlund, E. Lundberg, S. Navani, C. A.-K. Szigyarto, J. Odeberg, D. Djureinovic, J. O. Takanen, S. Hober, T. Alm, P.-H. Edqvist, H. Berling, H. Tegel, J. Mulder, J. Rockberg, P. Nilsson, J. M. Schwenk, M. Hamsten, K. von Feilitzen, M. Forsberg, L. Persson, F. Johansson, M. Zwahlen, G. von Heijne, J. Nielsen and F. Pontén, *Science*, 2015, **347**, 1260419.
5 A. Varki, *Trends Mol. Med.*, 2008, **14**, 351–360.
6 C. Frantz, K. M. Stewart and V. M. Weaver, *J. Cell Sci.*, 2010, **123**, 4195–4200.
7 K. C. Clause and T. H. Barker, *Curr. Opin. Biotechnol.*, 2013, **24**, 830–833.
8 Z. W. Chen, Q. Yu, L. Hao, F. B. Liu, J. Johnson, Z. C. Tian, W. J. Kao, W. Xu and L. J. Li, *Analyst*, 2018, **143**, 2508–2519.
9 S. Zhou, L. Veillon, X. Dong, Y. Huang and Y. Mechref, *Analyst*, 2017, **142**, 4446–4455.
10 Y. M. Hu and C. R. Borges, *Analyst*, 2017, **142**, 2748–2759.
11 B. Gerald, O. Bettina, G. Michael, S. W. Eric, B. S. Herbert and E. Oliver, *Eur. Respir. J.*, 2017, **50**, 1601805.
12 N. Komura, K. Kato, T. Udagawa, S. Asano, H.-N. Tanaka, A. Imamura, H. Ishida, M. Kiso and H. Ando, *Science*, 2019, **364**, 677–680.

13 W. H. Yang, P. V. Aziz, D. M. Heithoff, M. J. Mahan, J. W. Smith and J. D. Marth, *Proc. Natl. Acad. Sci. U. S. A.*, 2015, **112**, 13657–13662.
14 S. S. Pinho and C. A. Reis, *Nat. Rev. Cancer*, 2015, **15**, 540.
15 M. J. Schultz, A. F. Swindall and S. L. Bellis, *Cancer Metastasis Rev.*, 2012, **31**, 501–518.
16 J. C. Pickup, M. B. Mattock, M. A. Crook, G. D. Chusney, D. Burt and A. P. Fitzgerald, *Diabetes Care*, 1995, **18**, 1100–1103.
17 K. P. Gopaul and M. A. Crook, *Clin. Biochem.*, 2006, **39**, 667–681.
18 M. Ponnio, H. Alho, S. T. Nikkari, U. Olsson, U. Rydberg and P. Sillanaukee, *Clin. Chem.*, 1999, **45**, 1842–1849.
19 S. Hakomori, *Proc. Natl. Acad. Sci. U. S. A.*, 2002, **99**, 10231–10233.
20 A. Patel, S. Tiwari and P. K. Jha, *J. Biomol. Struct. Dyn.*, 2019, **37**, 1545–1554.
21 C. R. Bertozzi and L. L. Kiessling, *Science*, 2001, **291**, 2357–2364.
22 D. H. Dube and C. R. Bertozzi, *Nat. Rev. Drug Discovery*, 2005, **4**, 477.
23 K. Matsubara, Y. Matsushita, K. Sakai, F. Kano, M. Kondo, M. Noda, N. Hashimoto, S. Imagama, N. Ishiguro, A. Suzumura, M. Ueda, K. Furukawa and A. Yamamoto, *J. Neurosci.*, 2015, **35**, 2452–2464.
24 L. Frullano, J. Rohovec, S. Aime, T. Maschmeyer, M. I. Prata, J. J. P. de Lima, C. F. G. C. Geraldes and J. A. Peters, *Chem. – Eur. J.*, 2004, **10**, 5205–5217.
25 Y. Zhou, R. Aebersold and H. Zhang, *Anal. Chem.*, 2007, **79**, 5826–5837.
26 A. Arcinas, T.-Y. Yen, E. Kebebew and B. A. Macher, *J. Proteome Res.*, 2009, **8**, 3958–3968.
27 K. K. Palaniappan and C. R. Bertozzi, *Chem. Rev.*, 2016, **116**, 14277–14306.
28 J. A. Prescher, D. H. Dube and C. R. Bertozzi, *Nature*, 2004, **430**, 873–877.
29 D. E. Wang, J. H. Yan, J. J. Jiang, X. Liu, C. Tian, J. Xu, M. S. Yuan, X. Han and J. Y. Wang, *Nanoscale*, 2018, **10**, 4570–4578.
30 M. Y. Ji, P. Li, N. Sheng, L. L. Liu, H. Pan, C. Wang, L. T. Cai and Y. F. Ma, *ACS Appl. Mater. Interfaces*, 2016, **8**, 9565–9576.
31 Z. Y. Song, X. Liang, Y. D. Wang, H. B. Han, J. B. Yang, X. D. Fang and Q. S. Li, *Biomater. Sci.*, 2019, **7**, 1632–1642.
32 A. Liu, S. Peng, J. C. Soo, M. Kuang, P. Chen and H. Duan, *Anal. Chem.*, 2011, **83**, 1124–1130.
33 X. Wu, Z. Li, X.-X. Chen, J. S. Fossey, T. D. James and Y.-B. Jiang, *Chem. Soc. Rev.*, 2013, **42**, 8032–8048.
34 X. J. Yang, L. Zhou, Y. Hao, B. Zhou and P. H. Yang, *Analyst*, 2017, **142**, 2169–2176.
35 W. Cheng, L. Ding, Y. L. Chen, F. Yan, H. X. Ju and Y. B. Yin, *Chem. Commun.*, 2010, **46**, 6720–6722.
36 C. Zong, J. Wu, C. Wang, H. X. Ju and F. Yan, *Anal. Chem.*, 2012, **84**, 2410–2415.
37 F. Kisa, K. Yamada, T. Miyamoto, M. Inagaki and R. Higuchi, *Chem. Pharm. Bull.*, 2007, **55**, 1051–1052.
38 K. Sarkar, G. Madras and K. Chatterjee, *RSC Adv.*, 2015, **5**, 50196–50211.
39 M. Kunishima, C. Kawachi, K. Hioki, K. Terao and S. Tani, *Tetrahedron*, 2001, **57**, 1551–1558.
40 R. Okamoto, S. Souma and Y. Kajihara, *J. Org. Chem.*, 2008, **73**, 3460–3466.
41 R. M. Dirks and N. A. Pierce, *Proc. Natl. Acad. Sci. U. S. A.*, 2004, **101**, 15275–15278.
42 Y. L. Chen, L. Ding, T. T. Liu and H. X. Ju, *Anal. Chem.*, 2013, **85**, 11153–11158.
43 Y. M. Feng, Y. N. Guo, Y. R. Li, J. Tao, L. Ding, J. Wu and H. X. Ju, *Anal. Chim. Acta*, 2018, **1039**, 108–115.
44 P. Damborsky, K. M. Koczula, A. Gallotta and J. Katrlik, *Analyst*, 2016, **141**, 6444–6448.
45 S. Q. Li, Y. R. Liu, L. Liu, Y. M. Feng, L. Ding and H. X. Ju, *Angew. Chem., Int. Ed.*, 2018, **57**, 12007–12011.
46 W. Lin, Y. F. Du, Y. T. Zhu and X. Chen, *J. Am. Chem. Soc.*, 2014, **136**, 679–687.
47 C. G. Pierce, D. P. Thomas and J. L. López-Ribot, *J. Antimicrob. Chemother.*, 2009, **63**, 473–479.
48 H. P. Xiao, J. M. Smeekens and R. H. Wu, *Analyst*, 2016, **141**, 3737–3745.